Paper presented at "28th ESA Antenna Workshop on Space Antenna Systems and Technologies", 31 May-3 June 2005, ESTEC, Noordwijk, The Netherlands. Proceedings pp. 841-844.

SCATTERING FROM A LOW-ORBITING SATELLITE WITH ROTATING SOLAR ARRAY

Frank Jensen[(1)]

[(1)]*TICRA, Læderstræde 34, 2;DK-1204 Copenhagen K; Denmark; Email:ff@ticra.com*

ABSTRACT

The radiation patterns of satellite antennas may be highly influenced by scattering in the satellite, its payload and its solar array. By ray tracing techniques (GO/GTD) and applying orbit predicting data it is shown how it is possible to model the link signal to a given earth station taking into account that the solar array follows the direction to the sun and thus is rotating relative to the body of the satellite.

Predictions for the ENVISAT satellite are presented and compared to measured link signals.

The presented work is carried out for ESA on ESTEC contract 17875/03/NL/FF

1. INTRODUCTION

The signal from a satellite antenna may be influenced by scattering from the satellite payload as well as from the body of the satellite itself. Especially the wide radiation from the TTC antennas will be scattered. But severe scattering may also occur for medium gain antennas on low earth orbiting satellites which communicate with ground stations. The maximum gain requested for such antennas in directions of the horizon of the earth at 62º from nadir may cause a high illumination of scattering objects.

Due to its size, it is in particular the solar array which might shadow and reflect the antenna radiation. This adds a new dimension to the predictions as the orientation of the solar array is designed to follow the direction to the sun while the satellite itself is oriented towards the earth. The orientation of the solar array thus depends on the position in orbit of the satellite.

Geometrical ray tracing with application of GO (Geometrical optics) and GTD (Uniform Geometrical Theory of Diffractions) is very useful for such scattering predictions. For this, an extended version of GRASP9 has been applied. From a file the time varying distance and the relative orientation between the satellite and the ground station are read. This input includes the orientation of the solar array and is applied to rotate the array from time step to time step in the computations.

The method has been implemented for the European environmental satellite ENVISAT. The satellite geometry has been modelled and the link signal has been predicted for different passages of the Kiruna ground station. The results are compared to measurements of actual link signals.

2. GEOMETRY

ENVISAT is a 10 m long satellite with several payload instruments of which the 10 m wide panel of the Advanced Synthetic Aperture Radar (ASAR) is a major scattering element. To this adds the solar array which reaches out to 16 m from the satellite body, Fig. 1.

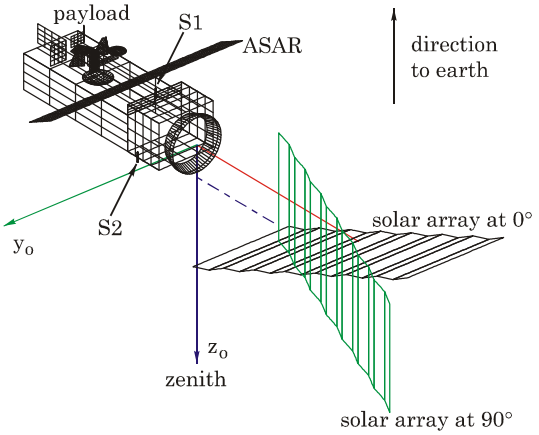

Figure 1. Electromagnetic model of the ENVISAT satellite with the solar array shown at 0º and 90º rotation.

3. S-BAND ANTENNAS

We will in the present paper consider the disturbances in the radiation of the 2.2 GHz TTC antennas. The satellite is equipped with two such antennas, S1 on the earth or nadir side of the spacecraft and S2 on the zenith side, Fig. 1. S1 is LHC polarised and S2 is RHC polarised. The antennas are fed with equal power.

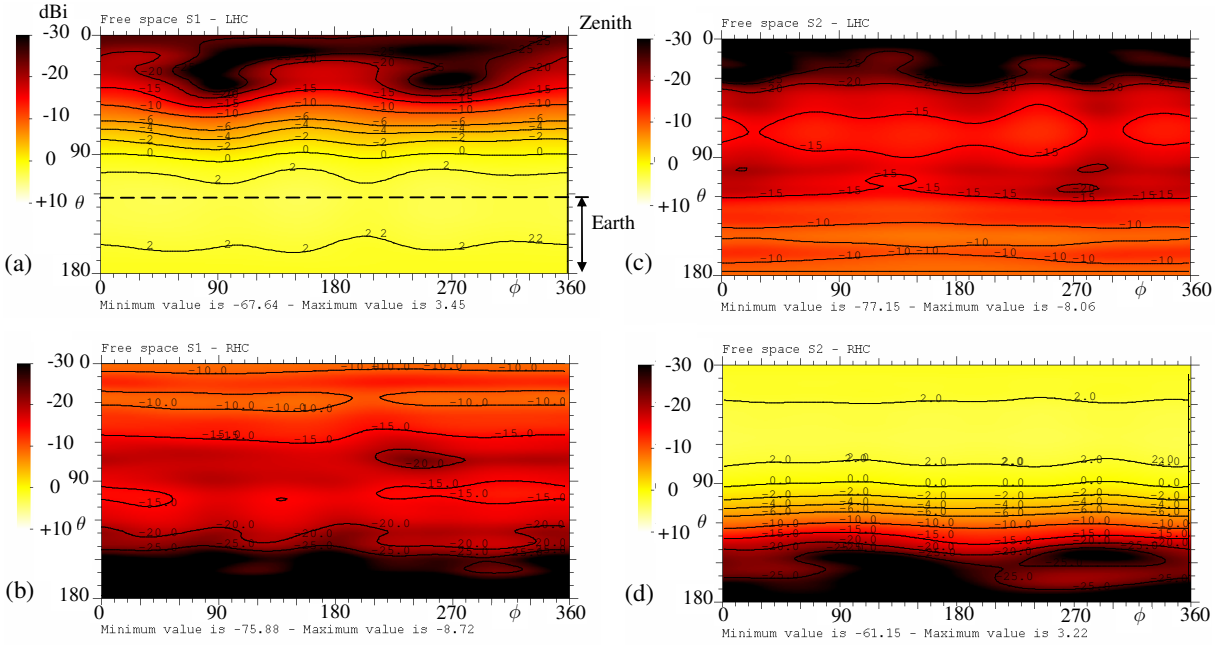

Figure 2. Free space patterns of S1 (left: a, b) and S2 (right: c, d) overlaid with contours in dBi. LHC, which is the co-polar polarisation on the lower hemisphere, is shown in the topmost part of the figure (a, c) and RHC is shown below (b, d).

The free-space co-polar (LHC) pattern of antenna S1 is given in Fig. 2a. This and the following patterns are presented in standard spherical (θ, ϕ)-coordinates in the satellite coordinate system which means that the earth is in the lower part of the diagram, namely for $117° \leq \theta \leq 180°$. The pattern is giving coverage over the hemisphere $90° \leq \theta \leq 180°$ (light colours in the figure; see the intensity scale at left side of the figures). It is thus this antenna which links to the earth stations and the polarisation of interest is the LHC.

The cross-polar (RHC) pattern of the antenna is shown in Fig. 2b. This is at a lower level but will interfere with the co-polar pattern if it is reflected in some scattering structure because RHC reflects as LHC.

The diagram of the other antenna, S2, is shown in Fig. 2c and 2d. Antenna S2 has a low LHC-radiation towards the earth and is furthermore shadowed by the satellite in these directions. The RHC pattern is strong in the upper hemisphere including the region $\theta \cong 90°$ in which the solar panel is situated.

4. ILLUMINATION ANALYSIS

When the antennas are mounted upon the satellite, the satellite geometry shadows (GO) as shown in black in Fig. 3a and 3b for antenna S1 and S2, respectively. The LHC component is shown shadowed here, cf. Fig. 2a and 2c.

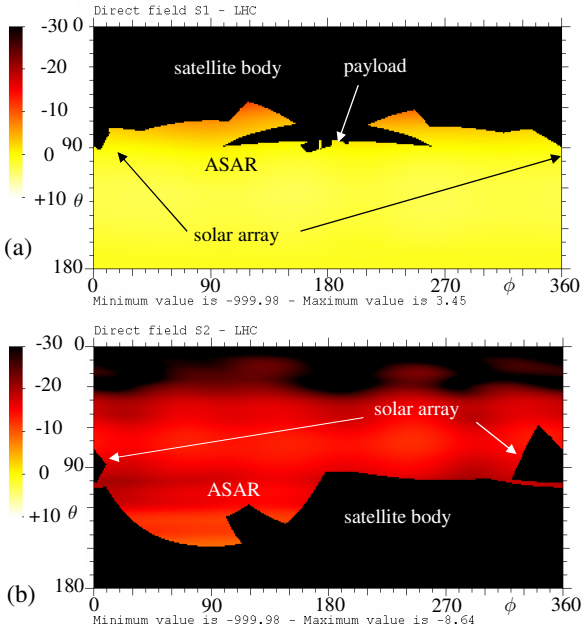

Figure 3. Direct earth illumination LHC patterns of S1 (a) and S2 (b). Shadowing elements are identified.

The shadowed parts of the RHC-patterns appear as reflections as shown in Fig. 4a and 4b (RHC field reflected as LHC), the body of the satellite giving the largest contribution. The solar array is rotated to the angle $\gamma = 61°$. Diffractions are so far not included.

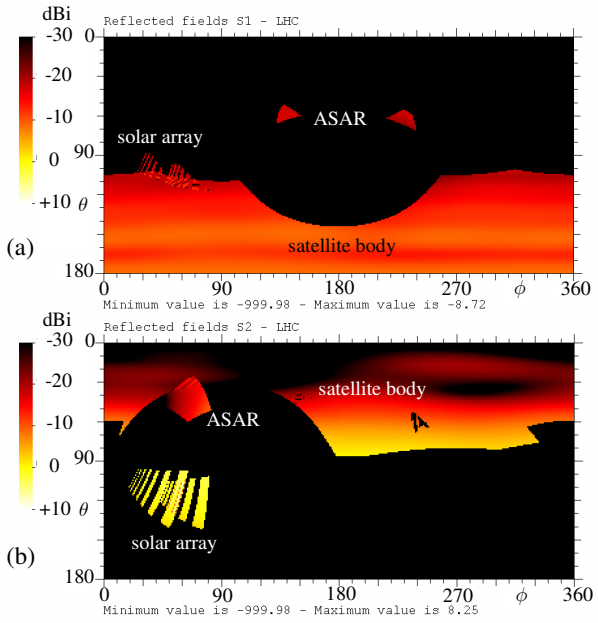

Figure 4. LHC patterns of reflections in satellite body, ASAR panel and solar array from S1 (a), and from S2 (b).

The total LHC field with all contributions added, direct, reflected and diffracted fields from both antennas, is shown in Fig. 5. This field is dominated by the direct antenna illumination (cf. Fig. 3a) but a strong influence of the reflections in the solar array (cf. Fig. 4b) is also seen. Furthermore, the diffractions causes ripples from interferences with the GO-field.

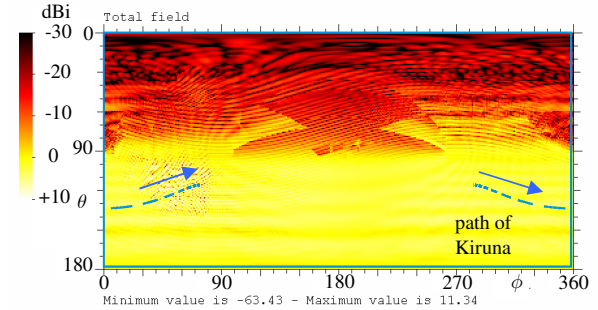

Figure 5. Total field in LHC. Shown is also (for a sample orbit) a path of Kiruna as seen from the satellite.

5. ORBIT CALCULATION

When the satellite passes an earth station then the direction to this station will describe a path over the satellites (θ,ϕ)-sphere. An example on such a path for Kiruna is shown in Fig. 5. The satellite flies in direction of its negative *y*-axis, $(\theta,\phi) = (90°,270°)$ and all paths starts near this direction and ends around $(\theta,\phi) = (90°,90°)$. For the chosen orbit, Kiruna is first seen at $(\theta,\phi) = (117°,285°)$, passes $\phi = 360°/0°$ and disappears at $(\theta,\phi) = (117°,75°)$. It is seen that the path crosses regions with reflections from S1 in the satellite body as well as from S2 in the solar array, Fig. 4. It is also seen from Fig. 3 that the direct field from S1 is not blocked while a direct signal from S2 only will occur during the late part of the passage ($30° \le \phi \le 75°$).

The path is given as a set of directions to Kiruna (one for each satellite position) at fixed time intervals. For each time the orientation of the solar panel is also given and the scattering may be computed for the geometry at this time as illustrated in the following figures.

In Fig. 6 we have depicted the GO contributions, namely the direct field from antenna S1 and the field from S1 reflected in the satellite body. These occur for the full passage. Further, we have the direct field from antenna S2 and the field from S2 reflected in the inner panels of the solar array (numbered from 1 and onward). These contributions occur only for the last part of the passage.

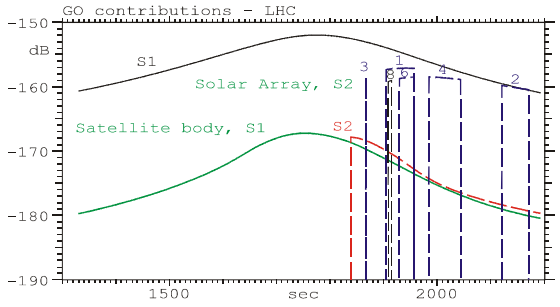

Figure 6. GO field contributions in LHC, direct fields from S1 (top solid curve, S1) and S2 (dashed curve, S2, starting at t = 1840 sec.) and reflections from the objects stated. Dashed curves are S2 contributions.

It is seen that the reflections from antenna S2 in the panels of the solar array are at levels comparable to the main field (the direct field from the earth oriented antenna, S1) and severe interference must be expected. The direct field from S2, as well as the field from S1 reflected in the satellite body, are 15-20 dB below the direct field of S1 and will only cause minor ripples in the main field from S1.

The GO contributions give an idea about the most significant field contributions. Correct contributions require the diffractions to be added, Fig. 7, but the general level of the field contributions are not changed.

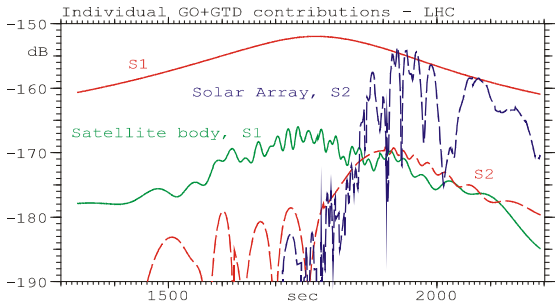

Figure 7. Diffractions are added to the GO fields giving the scattering, object by object (LHC). All contributions from the solar array are added to one scattering pattern.

Finally, the total field - given by adding all field contributions - is presented in Fig. 8 showing the severe disturbances during the last part of the passage.

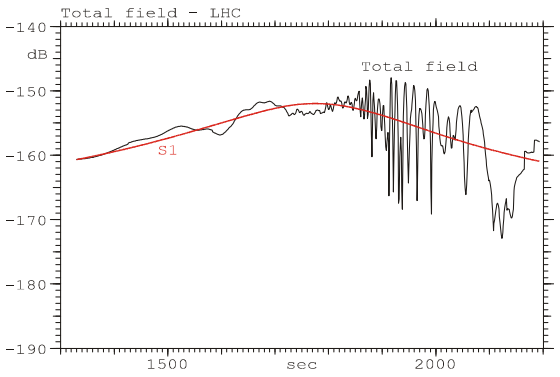

Figure 8. Total field (and direct field, S1, smooth red curve) obtained by adding all field contributions (LHC).

6. COMPARISON TO MEASURED LINK SIGNAL

The actually measured link signal for the modelled passage of Kiruna is given in Fig. 9.

A direct comparison to Fig. 8 is difficult due to a different presentation. Furthermore, measured radiation patterns for the actual antennas were not available and patterns for a similar antenna have been applied instead. Nevertheless, the overall time variation of the signal is very convincing. At the beginning of the passage the signal varies slowly in time with affordable amplitude variation but in the last third of the passage the signal becomes fast varying with deep nulls ending with two lobes of increasing widths, a performance which is readily recognized in the modelled field pattern.

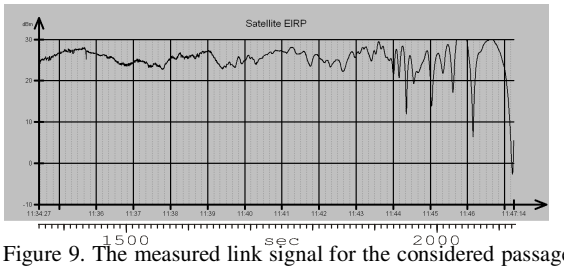

Figure 9. The measured link signal for the considered passage of Kiruna for the time interval 1360 < t < 2127 secs.

7. ILLUSTRATION OF THE RAYS

GO and GTD is a ray based technique and it is possible to visualize the individual ray paths contributing to the field. An example is given in Fig. 10 at the time t=1940 sec at which time reflections in panel 1 and 6 of the solar array occur, cf. Fig. 6. The solar array is here rotated to $\gamma = 61°$.

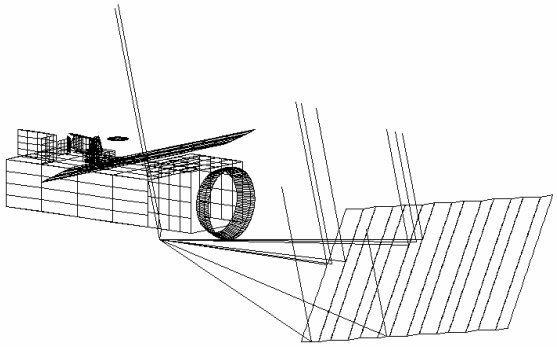

Figure 10. Rays in direction of Kiruna from antenna S2 at t=1940 sec. Direct ray and rays reflected and diffracted in the body of the space craft and in panel 1 and 6 of the solar array are shown. There are no diffractions in the upper edges of the solar panels as these edges are shadowed by the satellite body.

8. CONCLUSIONS

The direct and scattered fields of two S-band antennas on a satellite have been determined by conventional diffraction theory. The link signal for a given passage of an earth station has been modelled as function of time taking into account the rotation of the solar array. The result is in agreement with measured data.

A thorough understanding of the coverage of the individual ray contributions has been obtained by an intensive application of graphical tools.

The author thanks B. Duesmann of ESTEC for providing orbit data in satellite coordinates.